Physica D 288 (2014) 30–44

Contents lists available at ScienceDirect

Physica D

journal homepage: www.elsevier.com/locate/physd

Quasiperiodicity and phase locking in stochastic circle maps: A spectral approach

Alla Borisyuk*, Firas Rassoul-Agha

University of Utah, Department of Mathematics, 155 South 1400 East, Salt Lake City, UT 84112, USA

HIGHLIGHTS

- We study the Markov chain of consecutive spikes of periodically driven noisy neurons.
- We relate the dynamics of the Markov chain to the spectrum of its transition operator.
- Spectral spirals and zipping reveal quasiperiodicity and transition to phase-locking.
- Stochastic bifurcation regions are observed, rather than bifurcation points.
- Our method allows to predict dynamic regimes of noisy maps without direct simulation.

ARTICLE INFO

Article history:
Received 26 February 2013
Received in revised form
17 July 2014
Accepted 21 July 2014
Available online 14 August 2014
Communicated by K. Josic

Keywords:
Circle map
Markov chain
Stochastic matrix
Spectrum
Phase locking
Quasiperiodic

ABSTRACT

While there are clear definitions of what it means for a deterministic dynamical system to be periodic, quasiperiodic, or chaotic, it is unclear how to define such notions for a noisy system. In this article, we study *Markov chains* on the circle, which is a natural stochastic analog of deterministic dynamical systems. The main tool is spectral analysis of the transition operator of the Markov chain. We analyze path-wise dynamic properties of the Markov chain, such as stochastic periodicity (or phase locking) and stochastic quasiperiodicity, and show how these properties are read off of the geometry of the spectrum of the transition operator.

1. Introduction

Circle maps are by now standard and extensively studied objects in the theory of dynamical systems; see [1,2]. They are also widely used as models in many applications, e.g. cardiac arrhythmias (reviewed by Glass in [3]), the Schrödinger operator (see [4]), and neural systems (see [5–7]). Notions of phase locking, quasiperiodicity, and chaos, that describe the dynamics of such systems, are well defined and understood using tools such as the rotation number, bifurcation diagrams, and Feigenbaum diagrams; see [8–10].

Natural systems, however, are inherently noisy. Therefore, adding a stochastic component to the model makes it both more interesting and realistic. Introducing randomness compensates for lack of predictability in systems with a large number of degrees of freedom, such as gas molecules or neuronal networks.

Markov chains on the circle are a natural stochastic generalization of circle maps in that the evolution of the system only depends on its current state. However, the aforementioned tools, used to study deterministic systems, do not generalize in an obvious manner and new analytical methods are needed.

Markov chains are completely determined by their transition operators and it is widely believed that the spectra of those operators carry all the information about the chain's dynamics. Many aspects of these operators (such as mixing, asymptotic stability, etc.) have been extensively studied in the literature; see for example [11] and the review article [12]. It is well known that the spectral gap (i.e. the distance between the moduli of the top two eigenvalues) determines the speed of mixing of the chain. However, beyond that the rigorous connection between spectrum and dynamics is still an open problem. (For deterministic dynamical

* Corresponding author.
E-mail addresses: borisyuk@math.utah.edu (A. Borisyuk), firas@math.utah.edu (F. Rassoul-Agha).

http://dx.doi.org/10.1016/j.physd.2014.07.006
0167-2789/

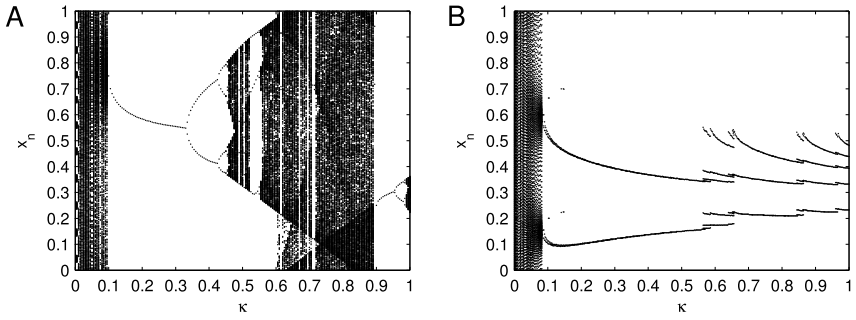

Fig. 1. Feigenbaum diagrams. (A) For the sine circle map with $a = 0.1$. (B) For the integrate-and-fire map with $\tau = 2$ and $I = 0.7$.

systems, the connection between spectral properties of the composition operators and ergodic and mixing properties of the systems has also been studied; see [13].)

Our work extends and complements earlier findings on real-complex transitions in the spectrum as indicators of changes in dynamics; see [14–21]. In these works the authors looked at properties of individual eigenvalues. In this work we assert that it is essential to consider the shape of the entire spectrum to more accurately predict the different aspects of the dynamics.

The article is organized as follows. In Section 2 we give an overview of circle maps and a discussion of Markov chains. We also provide examples of well-known circle maps and their stochastic analogs, namely sine-circle maps and the integrate-and-fire model. The deterministic versions of these examples are quite general in the sense that they have bifurcation scenarios that are ubiquitous throughout dynamical systems. In Section 3 we demonstrate how spectra and dynamics are related in the simpler setting of finite-state deterministic dynamical systems. In Section 4 we focus on the stochastic versions of the aforementioned examples and demonstrate how the dynamics of the Markov chain are related to the spectrum of its transition operator. We observe and explain spectral spirals in the quasiperiodic regime, "zipping" of the spectrum, and emergence and dominance of various phase-locked states. Then, in Section 5 we discuss our results and relate them to existing descriptions of changes in stochastic dynamics, such as P- and D-bifurcations and reliability. Finally, in Appendix A we justify the discretization of the Markov chain transition operator used in our numerics.

2. Setting

2.1. Deterministic dynamical systems: circle maps

A *circle map* is a function $F : \mathbb{R} \to \mathbb{R}$ satisfying $F(x+1) = F(x)+1$ for all x. It defines the map $f : \mathbb{S} \to \mathbb{S} : x \mapsto \{F(x)\}$ where $\{x\} = x - [x]$, $[x]$ is the largest integer smaller than x, and $\mathbb{S}$ is the circle $\mathbb{R}/\mathbb{Z}$ or, equivalently, the interval $[0, 1]$ with 0 and 1 identified. This in turn defines a *dynamical system* on $\mathbb{S}$, namely a sequence $x_{n+1} = f(x_n)$, where x_0 is the initial *state*. One is then interested in studying the behavior of the sequence (x_n); e.g. its periodicity, quasiperiodicity, ergodicity, support, invariant measures, dependence on x_0, etc. One quantity that is very useful in answering such questions is the so-called *rotation* (or *winding*) *number* $\rho = \lim_{n\to\infty} F^{(n)}(x_0)/n$, where $F^{(n)}$ is the nth iterate of F. Henri Poincaré proved that when f is orientation preserving this limit exists and is independent of the starting point x_0; see [22,23]. In this case, ρ is simply the number of times x_n wraps around $\mathbb{S}$ in a unit time. Then, when ρ is rational, the dynamical system is said to be *periodic* (or *phase locked*). In this case, starting at Lebesgue-almost every point x, x_n will eventually converge to a periodic orbit. When the rotation number is irrational the system is *quasiperiodic* and the orbit is either dense in $[0, 1]$ (if, for example, F is continuous) or converges to a Cantor set; see [8,24]. In the more complicated situation of circle maps that are not orientation preserving the limit defining ρ may not exist and the limsup and liminf could depend on the starting point. When this happens, the system becomes sensitive to the slightest perturbation of the initial condition and is said to be *chaotic*; see [25]. General overview of these topics can be found in [9,10,1,2].

Usually, there are also one or more parameters on which f depends; i.e. we have a family $f_\kappa(x)$. Then, one asks about how the behavior of (x_n) depends on the parameter κ. *Feigenbaum diagrams* (similar to *bifurcation diagrams*) allow to visualize the behavior of (x_n) by tracking the *attractors* of the system, as functions of κ. Even circle maps that have very simple expressions can exhibit a wide range of interesting behavior.

The next two examples are in the context of neural spiking, where we think of x_n as the phase of the nth spike relative to the sinusoidal external forcing. The map then takes the phase of the current spike within the forcing cycle and transforms it into the phase of the subsequent spike.

Example 2.1 (*Sine Circle Map*)**.** Given $a \in [0, 1)$ let

$$F_\kappa(x) = x + a + \kappa \sin(2\pi x) \quad \text{and} \quad f_\kappa(x) = \{F_\kappa(x)\}.$$

As $\kappa > 0$ varies, the corresponding dynamical system switches from being essentially quasiperiodic ($0 < \kappa < a$) to having one stable and one unstable fixed points ($a < \kappa < \sqrt{a^2 + 1/\pi^2}$) to having a limit cycle of two points, then four, etc., until the onset of a chaotic regime. (This is the so-called *period-doubling route to chaos*.) After that comes a fractal-like sequence of periodic and chaotic regions. The Feigenbaum diagram appears in Fig. 1(A). See Section 4 for some more details.

Example 2.2 (*Periodically-Driven Integrate-and-Fire*)**.** Given $s \in [0, 1)$ and $I \in \mathbb{R}$ consider the equation

$$\frac{dV}{dt}(t; s) = -\frac{1}{\tau}V(t; s) + I + \kappa \sin(2\pi t), \quad t \geq s;$$
$$V(s; s) = 0.$$

Let $F_\kappa(s) = \inf\{t > s : V(t; s) > 1\}$ and $f_\kappa(s) = \{F_\kappa(s)\}$, the first time (mod 1) $V(\cdot\,; s)$ reaches the threshold level 1. (If the threshold is not reached, the system is said to have been *quenched* and F_κ is set to infinity. This does not happen if I is large enough.) V models the membrane potential of a neuron. It starts at a reset level, assumed 0 here, and increases until it reaches a threshold level, which we assumed to equal 1. When that level is reached the neuron is said to have *fired* and the potential is reset. The dynamical system of interest is then the sequence of firing times. Since the stimulus $\kappa \sin(2\pi t)$ has been chosen to have period 1, the firing times are considered modulo this period, in which case we have a discrete-time dynamical system on the circle. This system has been shown to switch from quasiperiodic to periodic behavior as the parameter increases (Fig. 1(B); [5]).

Variants of the above integrate-and-fire model have also been considered in [6]. The resulting circle maps are similar to the ones mentioned in the above two examples.

2.2. Stochastic dynamical systems: Markov chains—definition and examples

As was mentioned in the Introduction, in some contexts it is important to include a stochastic component in the system. Adding noise may drastically change the system's behavior; e.g. the dynamical system $X'(t) = \alpha - X(t)^2$ exhibits the so-called saddle–node bifurcation as α changes sign, while the stochastic counterpart $dX(t) = (\alpha - X(t)^2)dt + \sigma dB(t)$ (where $B(t)$ is standard Brownian motion) becomes such that with probability one $X(t) \to -\infty$ in finite (albeit random) time regardless of the values of α or the starting point. Noise endows the system with new properties such as increased or decreased stability, reliability or unreliability, and larger range of responses. In neuroscience in particular, noise in neuronal systems has recently been receiving a lot of attention. Nervous systems seem to have developed many ways to counteract the noise, and also multiple ways to use it to their benefit. For examples and reviews see [26–31].

In this work, we will focus on a particular type of stochastic processes, namely Markov chains (X_n) on the circle $\mathbb{S}$ (endowed with its Borel σ-algebra). For such processes, the distribution of the next position X_{n+1} only depends on the value of the current position X_n, as opposed to the whole history $X_0, \dots, X_n$. Subsequently, Markov chains on the circle are a natural stochastic generalization of circle maps.

A Markov chain is completely determined by its *transition operator* that maps bounded continuous functions to bounded measurable ones:

$$\Pi : \mathscr{C}(\mathbb{S}) \to L^\infty(\mathbb{S}) : h \mapsto \Pi h(x) = E_x[h(X_1)], \tag{2.1}$$

where $E_x[h(X_1)]$ is the average value of $h(X_1)$ given $X_0 = x$.

Example 2.3. Let F be a circle map. Let $\sigma > 0$ and (ξ_n) be a sequence of independent identically distributed (i.i.d.) random variables. Set $X_{n+1} = \{F(X_n) + \sigma\xi_{n+1}\}$. Here, $\Pi h(x) = E[h(\{F(x) + \sigma\xi_1\})]$.

As a special case, one can take F to be as in Examples 2.1 or 2.2. When also ξ_i are standard normal we call the former the *stochastic sine circle map* model and the latter the *simplified stochastic integrate-and-fire* model.

Another (in a sense more natural) way to introduce noise to the integrate-and-fire model is as follows.

Example 2.4 (*Stochastic Integrate-and-Fire*)**.** Fix $\sigma > 0$. Given time $s \in [0, 1)$ consider the stochastic differential equation

$$dV(t; s) = \left(-\frac{1}{\tau}V(t; s) + \kappa \sin(2\pi t) + I\right) dt + \sigma\, dB(t), \quad t \geq s;$$
$$V(s; s) = 0.$$

(Recall that $B(t)$ is standard Brownian motion.) Given a starting time $s \in [0, 1)$ define the Markov chain (T_n) of (folded) neuron firing times as follows: $T_0 = s$ and for $n \geq 0$, $T_{n+1} = \{\inf\{t : t > T_n, V(t; T_n) > 1\}\}$. Here, $\Pi h(s) = E_s[h(T_1)]$.

It is noteworthy that when the noise in Example 2.4 is small, i.e. $\sigma \ll 1$, the Markov chain stays very close to the one in Example 2.3 with a possibly different but still small σ, function F corresponding to Example 2.2, and variables ξ_i i.i.d. standard normal; see [14]. Hence the name "simplified" stochastic integrate-and-fire. The advantage of using the model in Example 2.3 is just that it is easier to simulate.

Throughout the paper, we will assume that transition operator Π has a transition density (or kernel) $p(y|x)$ relative to Lebesgue measure:

$$\Pi h(x) = \int_0^1 p(y|x)h(y)\, dy.$$

Heuristically, $p(y|x)dy$ is the probability of the Markov chain jumping to $(y, y+dy)$, given it is currently observed at x. This assumption is satisfied in the case of Example 2.3 when variables ξ_n themselves have a density relative to Lebesgue measure. In this case $p(y|x)$ has an explicit formula in terms of the density of the ξ-variables. Our assumption is also satisfied in the case of Example 2.4. Here, however, $p(y|x)$ is not explicit. It satisfies a Volterra integral equation that can be solved numerically, e.g. following the scheme described in [32].

Since the state space of the Markov chain is compact, there exists at least one *invariant measure* μ, i.e. a measure μ such that $\mu\{X_1 \in A\} = \mu\{X_0 \in A\}$ for all measurable sets A. (If X_0 has distribution μ, then so does X_n for all $n \geq 1$.) When $p(y|x) > 0$ for Lebesgue-almost every x and y, this invariant measure is unique, i.e. there is no multistability. This measure is also ergodic, i.e. $\Pi h(x) = h(x)$ for μ-almost every x implies the existence of a constant c such that $h(x) = c$ for μ-almost every x; see for example Theorem 10.0.1 of [33]. Furthermore, measure μ is supported on the whole interval $[0, 1]$ and is mutually absolutely continuous relative to Lebesgue measure; see for example Theorem 10.4.9 of [33].

2.3. Stochastic dynamical systems: Markov chains—dynamics

It is an interesting and hard question to classify how the different ways of adding noise to a dynamical system affect the resulting dynamic behavior. It is in fact not always clear how to even define the stochastic counterparts of phenomena such as phase locking, quasiperiodicity, and chaos.

For instance, even when the system is ergodic and the rotation number ρ exists and is independent of the starting point, it often depends continuously on the strength of the noise and thus does not quite expose a periodic, quasiperiodic, or chaotic behavior, contrary to the deterministic case. To illustrate in a simple example, consider the Markov chain Y_n on $\mathbb{R}$ with transitions

$$\pi_{n,n+1/3} = \pi_{n+1/3,n+2/3} = 1 \quad \text{and}$$
$$\pi_{n+2/3,n+4/3} = 1 - \pi_{n+2/3,n+1} = \varepsilon \in (0, 1),$$

for $n \in \mathbb{Z}$, and $\pi_{x,[x]+1} = 1$ for any $x \notin \mathbb{Z}/3$. The corresponding Markov chain X_n on the state space $[0, 1)$ has transitions $\pi_{0,1/3} = \pi_{1/3,2/3} = 1, \pi_{2/3,1/3} = 1 - \pi_{2/3,0} = \varepsilon$, and $\pi_{x,0} = 1$ for $x \notin \{0, 1/3, 2/3\}$. (For Markov chain Y_n, $\pi_{x,y}$ is the probability that it will transition from location x to location y. In the case of X_n, the subscripts are locations folded relative to a period of 1.)

Markov chain X_n has a unique invariant measure concentrated at 0, 1/3, and 2/3 with weights equal to $(1-\varepsilon)/(3-\varepsilon)$, $1/(3-\varepsilon)$, and $1/(3-\varepsilon)$ respectively. (In other words, if X_0 is chosen according to this measure, then X_n has the same distribution for all $n \geq 0$.) The rotation number for X_n is inherited from Y_n and by the ergodic theorem equals the average increment of chain (Y_n) once it has reached stationarity: $\lim_{n\to\infty} Y_n/n = E[Y_1]$. However, once stationary, (Y_n) has increment 2/3 a fraction $\varepsilon \times 1/(3-\varepsilon)$ of the time and 1/3 a fraction $1 - \varepsilon \times 1/(3-\varepsilon)$ of the time. Hence, the rotation number equals $2/3 \times \varepsilon/(3-\varepsilon) + 1/3 \times (3-2\varepsilon)/(3-\varepsilon) = 1/(3-\varepsilon)$.

Clearly, we can choose ε as small as we wish and have $\rho \notin \mathbb{Q}$ or $\rho \in \mathbb{Q}$ at will. However, as $\varepsilon \to 0$ the Markov chain becomes very similar to a deterministic system of period 3.

Remark 2.5. Although the above example is highly singular, it can be modified so that Π does have a smooth density $p(y|x)$ and still have the rotation number ρ be rational or irrational as desired.

On the other hand, the stochastic analog of a fixed-point bifurcation is useful for studying the dynamics of random dynamical systems. One stochastic counterpart of a fixed point is an *invariant measure*. As was pointed out at the end of Section 2.2, the systems

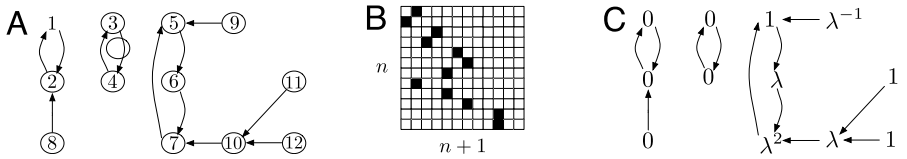

Fig. 2. (A) A map with $N = 12$ showing $\mathscr{C}_1 = \{1, 2\}$, $\mathscr{C}_2 = \{3, 4\}$, $\mathscr{C}_3 = \{5, 6, 7\}$, $\mathcal{T}_1 = \{8\}$, $\mathcal{T}_2 = \varnothing$, $\mathcal{T}_3 = \{9, 10, 11, 12\}$, $\mathcal{T} = \{8, 9, 10, 11, 12\}$, and the leaves are $\{8, 9, 11, 12\}$. (B) The corresponding 12×12 matrix (unitary entries are shaded). (C) An eigenvector corresponding to an eigenvalue λ with $\lambda^3 = 1$.

we consider have a unique invariant measure. Still, one may define a stochastic bifurcation (called *pathological- or P-bifurcation*, [34]) as the point where a qualitative change in the invariant measure takes place. For example, as the parameter crosses a value, the probability density function of this measure may switch from having one peak to having two peaks.

Another stochastic counterpart of a fixed point is the so-called *random attractor*. Roughly speaking, the stochastic bifurcation called *dynamic- or D-bifurcation* occurs when the system switches from being *reliable* (i.e. paths with different initial states converge as $n \to \infty$) to being *unreliable* (i.e. paths do not converge), or vice versa; see [34] and Definition 5.4 of [35].

There is no unique way to define a stochastic bifurcation. For instance, it is possible in general to construct examples where both of the above types occur or only one type of bifurcation occurs. See Chapter 9 of [34] for examples in the context of stochastic differential equations.

The situation in a stochastic system is further complicated by the fact that it exhibits different dynamics at different time scales. For instance, an ergodic Markov chain on $\mathbb{S}$ will revisit and get as close as we wish to any piece of any given orbit, no matter how long the piece is, infinitely many times. In other words, the Markov chain will look at times as if it is periodic of period 2, and at other times will seem to have period 5, and at others will seem quasiperiodic or chaotic, and so on. Of course, each such behavior comes with a likelihood value and the dynamics of interest are the ones that are "more likely" to occur. This brings us to the subject of the current work.

In Appendix A we show that under suitable assumptions transition operator Π has countably many nonzero eigenvalues with finite multiplicities. In Section 4 we relate the various dynamic regimes of the Markov chain to this spectrum. But first we start with the simpler situation of deterministic finite-state dynamical systems. In the next section, we show how these can be represented by a matrix and how the dynamics of the system are intimately related to the spectral properties of the associated matrix.

Although we do not use deterministic systems to deduce any properties about the stochastic operators we analyze in Section 4, the results of the following section guide us and provide insights in the course of our analysis.

3. Finite-state dynamical systems: circle map matrices

Throughout this section N will be a fixed natural number and we consider dynamical systems on N states, i.e. maps from $\{1, \dots, N\}$ into itself. Such maps arise as discretizations of circle maps, by binning the circle $\mathbb{S}$ into N equal intervals. (To continue the analogy with spiking systems, think of the situation where the forcing period is divided into N bins and instead of spike times only the bin numbers from 1 to N are recorded.)

Let us justify our use of the term "circle map *matrix*" in the title of the section. Observe that there is a one-to-one correspondence between maps from $\{1, \dots, N\}$ into itself and $N \times N$ matrices with entries in $\{0, 1\}$ and such that each row has exactly one entry equal to 1. Indeed, given such a matrix, each $i \in \{1, \dots, N\}$ maps to the unique integer j such that $\pi_{i,j} = 1$, and vice-versa. We will thus abuse notation and use π for both objects. See Figs. 2(A) and (B).

When N is small it is quite simple to deduce the dynamics of the system by looking directly at the matrix itself and no spectral analysis is really necessary. However, when N is large this is no longer possible. The objective of this section is to determine which features of the spectrum are responsible for the different aspects of the dynamics.

Let π be a map from $\{1, \dots, N\}$ into itself. This map induces a dynamical system: each point $i \in \{1, \dots, N\}$ *flows* into $\pi(i)$. We will use $\pi^n(i)$ to denote the image of i under n applications of the map π. Under the action of the map π, $\{1, \dots, N\}$ can be split into a *transient* part

$$\mathcal{T} = \{i : \pi^n(i) \neq i \,\forall n \geq 1\}$$

and a finite collection of disjoint *cycles* (or *irreducible components*) $\mathscr{C}_1, \dots, \mathscr{C}_k$: $\forall i \in \mathscr{C}_\ell \; \exists n \geq 1$ such that $\pi^n(i) = i$ and $\mathscr{C}_\ell = \{\pi^m(i) : m \geq 0\}$.

We show an example of such a map in Fig. 2 with $N = 12$. Panel A shows the possible transitions under the map and panel B the corresponding matrix with zero entries shown in white and entries of one are shaded. Each row i of the matrix has exactly one nonzero (shaded) entry in column j such that $\pi(i) = j$.

Let p_ℓ be the cardinality of $\mathscr{C}_\ell$, i.e. the length of the cycle. Then each cycle $\mathscr{C}_\ell$ is of the form $\{x_0, \dots, x_{p_\ell - 1}\}$ with $\pi(x_0) = x_1, \dots, \pi(x_{p_\ell - 2}) = x_{p_\ell - 1}$, and $\pi(x_{p_\ell - 1}) = x_0$.

$\mathcal{T}$ can be further split into disjoint transients that eventually flow into the different cycles:

$$\mathcal{T}_\ell = \{i \in \mathcal{T} : \exists n \geq 1 \text{ such that } \pi^n(i) \in \mathscr{C}_\ell\}.$$

A point $i \in \mathcal{T}$ is called a *leaf* if $\nexists j$ such that $\pi(j) = i$. Leaves of $\mathcal{T}$ correspond to 0 columns of π. Thus $\mathcal{T}$ is empty if and only if π has no 0 columns. When $\mathcal{T}$ is empty, π is a bijection and the corresponding map is a permutation of $\{1, \dots, N\}$.

As can be seen from Fig. 2(A), in this example $\mathscr{C}_1 = \{1, 2\}$, $\mathscr{C}_2 = \{3, 4\}$, $\mathscr{C}_3 = \{5, 6, 7\}$, $\mathcal{T}_1 = \{8\}$, $\mathcal{T}_2 = \varnothing$, $\mathcal{T}_3 = \{9, 10, 11, 12\}$, $\mathcal{T} = \{8, 9, 10, 11, 12\}$, and the leaves are $\{8, 9, 11, 12\}$.

Let π be the circle map $N \times N$ matrix corresponding to the map π as described above (Fig. 2(B)). We will identify a vector $v \in \mathbb{C}^N$ with a function $v : \{1, \dots, N\} \to \mathbb{C}$ in the obvious way.

Note that if $v = (v(1), \dots, v(N))$, then $\pi v = (v(\pi(1)), \dots, v(\pi(N)))$ or, in other words, $\pi v(x) = v(\pi(x))$. We denote the transpose of π by π^*. If v is such that $v(j_0) = 1$ and $v(j) = 0$ for $j \neq j_0$, then $(\pi^*)^i v$ is a vector that has a 1 at the $\pi^i(j_0)$th coordinate and 0 elsewhere. In other words, matrix π^* flows the mass according to the map π. (This in fact explains why in the physics literature π^* is sometimes called the transition matrix, rather than π.)

Recall that the *geometric multiplicity* of an eigenvalue λ is the dimension of the corresponding eigenspace $\mathscr{E}_\lambda(\pi)$. The *algebraic multiplicity* is the multiplicity in the characteristic polynomial $\det(\pi - \lambda I)$. The algebraic multiplicity is always larger than or equal to the geometric multiplicity.

The following lemma fully describes the spectra and eigenspaces of circle map matrices π and their connection to the dynamics (i.e. the cycles and transients) of the corresponding maps π.

Lemma 3.1. *The following hold about π.*

(a) *The spectrum of π consists of the union of all the roots of $\lambda^{p_\ell} = 1$, $1 \le \ell \le k$, and, if $\mathcal{T} \neq \varnothing$, of 0. (Recall that k is the number of cycles and $p_1, \dots, p_k$ their lengths.)*

(b) *Eigenvectors corresponding to eigenvalue $\lambda \neq 0$ with $\lambda^p = 1$ can be obtained by setting v to 1 at any x_0 in a cycle of length p then using $v(\pi(x)) = \lambda v(x)$ to define v on the rest of the cycle and at any points in $\mathcal{T}$ eventually mapping into the cycle. On the rest of the points v is set to 0 (Fig. 2(C)).*

(c) *An eigenvalue $\lambda \neq 0$ has geometric multiplicity equal to the number of cycles of length p with $\lambda^p = 1$. The geometric and algebraic multiplicities are equal for such eigenvalues. Consequently, the projection of the matrix onto the corresponding eigenspace is diagonalizable. (In particular, eigenvalue 1 has geometric and algebraic multiplicities k, the number of disjoint cycles.)*

(d) *If $\mathcal{T}$ is not empty, eigenvectors corresponding to eigenvalue 0 are obtained by setting v to 1 at a leaf of $\mathcal{T}$ and 0 elsewhere.*

(e) *If $\mathcal{T}$ is not empty, eigenvalue 0 comes with geometric multiplicity equal to the number of leaves of $\mathcal{T}$. This is the same as the number of 0 columns of π. Its algebraic multiplicity equals the cardinality of $\mathcal{T}$.*

Proof. First, observe that the matrix π can be diagonalized into ℓ blocks each corresponding to a set $\mathcal{T}_\ell \cup \mathscr{C}_\ell$. Thus, it is enough to consider the case of one cycle of length p and one transient $\mathcal{T}$ eventually flowing into $\mathscr{C}$ under the action of π.

Next, notice that if $\pi v = \lambda v$, $\lambda \neq 0$, and $\mathscr{C} = \{x_0, \dots, x_{p-1}\}$ as explained above, then $v(x_i) = \lambda^i v(x_0)$ for $0 \le i \le p-1$ and either $\lambda^p = 1$ or $v \equiv 0$ on the whole cycle. In the latter case, $v(\pi(x)) = \pi v(x) = \lambda v(x)$ for all x implies $v \equiv 0$ on $\mathcal{T}$ as well. On the other hand, if $\pi v = 0$, then $v(\pi(x)) = 0$ for all x and thus $v(y)$ can only be nonzero if y is a leaf of $\mathcal{T}$. Claims (a), (b), and (d) now follow. Since we only have one cycle of length p, the p nonzero eigenvalues are simple and claims (c) and (e) follow. □

Remark 3.2. Since the geometric and algebraic multiplicities may differ for $\lambda = 0$, diagonalizing the corresponding part of π may result in a number of nilpotent blocks (the Jordan decomposition). The number of these blocks equals the number of leaves of $\mathcal{T}$ and the length of the different blocks is determined by the length of the different branches of $\mathcal{T}$.

Let us now illustrate the lemma using the example in Fig. 2. The spectrum of the matrix consists of -1 with multiplicity 2, 1 with multiplicity 3, $e^{\frac{2\pi i}{3}}$ and $e^{-\frac{2\pi i}{3}}$ with multiplicity 1 each, and of zero with algebraic multiplicity 5. Parts (a), (c) and (e) of the lemma imply then that the total number of cycles is 3 (the multiplicity of eigenvalue 1), that there are two cycles of length 2, one cycle of length 3, and that there are 5 transient states. The geometric multiplicity of eigenvalue 0, which equals the number of zero columns in the matrix, is 4. Hence there are four leaves in the system.

According to part (b) of the lemma the eigenvectors for nonzero eigenvalues can be found by starting somewhere at the cycle of corresponding length, setting 1 there and then proceeding forward and backward, respectively multiplying and dividing by λ, and then setting all the other connected components to zero. This is illustrated in Fig. 2(C) for a λ with $\lambda^3 = 1$ (which hence corresponds to a cycle of length 3). The resulting eigenvector is $(0, 0, 0, 0, 1, \lambda, \lambda^2, 0, \lambda^{-1}, \lambda, 1, 1)$. Non-zero entries of each eigenvector point out a connected component of the network.

According to part (d) eigenvectors corresponding to eigenvalue zero have a one at a leaf and zeros elsewhere. In the example (0, 0, 0, 0, 0, 0, 0, 0, 0, 0, 0, 1) is one such eigenvector, since 12 is a leaf.

Next, we describe the spectrum and eigenspaces (associated to nonzero eigenvalues) of the adjoint (or transpose) of a circle map matrix. (The eigenvectors associated to eigenvalue 0 are also possible to describe, though we omit them.)

Lemma 3.3. *The following hold about π^*.*

(a) *The spectrum of π^* is the same as that of π, with the same multiplicities.*

(b) *Eigenvectors corresponding to eigenvalue $\lambda \neq 0$ with $\lambda^p = 1$ can be obtained by setting v to 1 at some x_0 in a cycle of length p then using $v(x) = \lambda v(\pi(x))$ to determine v along the cycle, and setting v to 0 outside the cycle.*

Part (a) is a known fact about real matrices. The proof of part (b) is similar to that of the previous lemma and is thus omitted. (Observe that $\pi^* v(x) = \sum_{y:\pi(y)=x} v(y)$, with the usual convention that a sum over an empty set is 0.)

Recall that π^* flows mass forward. Thus, the eigenvectors of π^* corresponding to $\lambda = 1$ give the invariant measures of the Markov chain with transition matrix π. The main (extreme, ergodic) ones are the uniform measures on each cycle (thus, k of them) and all other invariant probability measures are simply convex combinations of these.

One useful consequence is that an orthogonal system of eigenvectors of π^* corresponding to $\lambda = 1$ reveals the different cycles: each eigenvector consists of ones on the cycle and zeros elsewhere.

If we consider sites $\{1, \dots, N\}$ to be ordered in the natural way, then even if we know the cycle lengths, cycles of the same length may differ in the way their elements are ordered. For example, the cycle $1 \mapsto 3 \mapsto 2 \mapsto 1$ is different from the cycle $1 \mapsto 2 \mapsto 3 \mapsto 1$, even though they both have period (or length) 3. The difference is that the first cycle crosses the set $\{1, 2, 3\}$ twice before its completion (i.e. requires two periods), while the second cycle crosses it only once before completion (i.e. requires one period). We thus say the former cycle is 2:3 (two-to-three) while the latter is 1:3 (one-to-three). In general a cycle is q:p if q periods are needed to complete the cycle of length p.

To track down the different q:p cycles we can find an orthogonal system of eigenvectors of π^* corresponding to (any) $\lambda \neq 1$ with $\lambda^p = 1$ and p being the length of the cycle in question. After normalizing each vector to have an entry equal to 1, powers of λ^{-1} indicate the successive elements of the cycle. $q-1$ then is the number of times we encounter $\pi(x) < x$ along the cycle.

Remark 3.4. If the map on $\{1, \dots, N\}$ is induced by folding an integer-valued dynamical system with positive increments, then the notion q:p can also be introduced in the original (unfolded) process, but then q may get larger by the number of periods skipped during the cycle. For example, the unfolded version of $1 \mapsto 2 \mapsto 3 \mapsto 1 \mapsto \cdots$ requires crossing the cycle at least once, but possibly more if some cycles are skipped completely. Thus, the actual (unfolded) value of q cannot be determined from the folded map.

4. Stochastic circle maps: dynamics and spectrum

We now return to our earlier discussion of Markov chains on the circle. By the discussion in Appendix A, the transition operator Π defined by (2.1) is a compact operator. It thus has a discrete spectrum with the nonzero (countably many) eigenvalues having finite multiplicities and possibly accumulating at 0; see Theorem 6.26 of Chapter 3 of [36].

The purpose of this section is to relate this spectrum to the dynamics of the Markov chain. For now we will focus our discussion on the concrete context of the stochastic sine circle map in Example 2.3. In Sections 4.8 and 4.9 we will briefly discuss the other two models of integrate-and-fire. Let us recall the setting: $a \in [0, 1)$, $f_\kappa(x) = x + a + \kappa \sin(2\pi x)$, $X_{n+1} = f_\kappa(X_n) + \sigma\xi_n$, and ξ_n i.i.d. standard normal random variables.

To get a sense of things to come we invite the reader to watch the movie associated with Fig. 3(A). It shows the spectrum and dynamics of the stochastic system as parameter κ is varied. In the

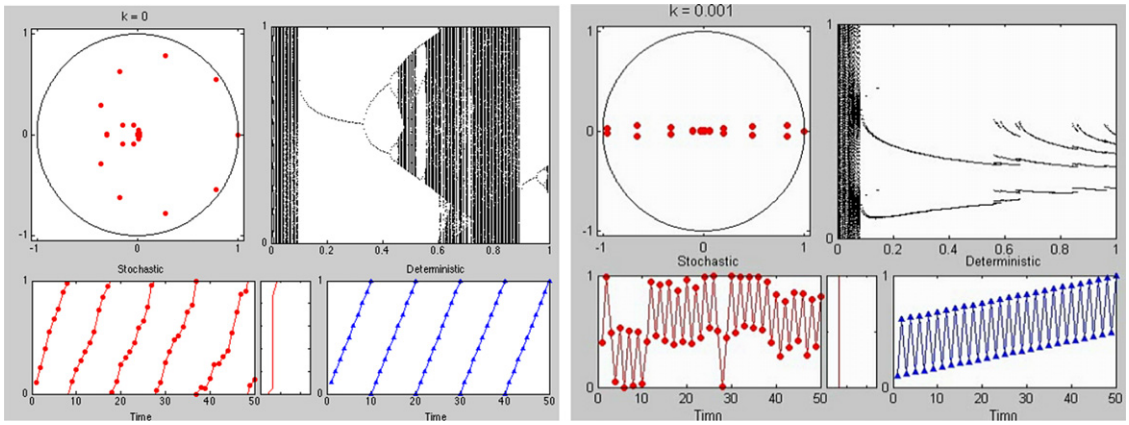

Fig. 3. Videos showing the spectrum (upper left), Markov chain dynamics (lower left), invariant measure (lower middle), Feigenbaum diagram (upper right), and deterministic dynamics (lower right). Left: For the sine circle map with parameters $a = 0.1$ and $\sigma = 0.05$; see supplementary file `mmc1.mp4`. Right: For the integrate-and-fire map of Example 2.4 with parameters $I = 0.7$, $\tau = 2$, and $\sigma = 0.01$; see supplementary file `mmc2.mp4`. Files are available at http://dx.doi.org/10.1016/j.physd.2014.07.006. A video for the simplified integrate-and-fire model of Example 2.3 (`mmc2.mp4`) is also available at this website (see Appendix B).

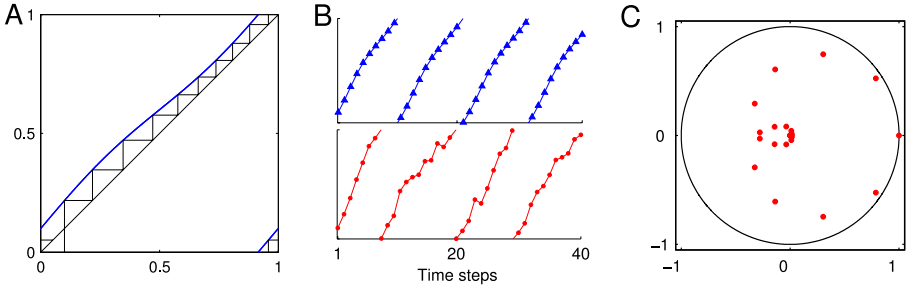

Fig. 4. (A) Sine circle map with $a = 0.1$ and $\kappa = 0.03$ and the first few steps of cobwebbing of sequence (x_n) with $x_0 = 0.1$. (B) Upper: Deterministic sequence (x_n); Lower: Markov chain (X_n) with $\sigma = 0.05$. Both sequences are wrapping densely around $\mathbb{S}$ and are hence quasiperiodic. (C) The spectrum of Π exhibiting the spirals.

video (see Appendix B), parameters a and σ are set to 0.1 and 0.05 respectively. The top left panel shows the spectrum of the stochastic system, a sample trajectory (with $X_0 = 0.1$) is in the lower left panel, and the middle panel shows the corresponding invariant measure. The right panels show the dynamics with the same κ in the deterministic case ($\sigma = 0$). The type of dynamics can be read off of the Feigenbaum diagram in the top panel or from observing a sample trajectory in the lower panel, where $x_0 = 0.1$. The goal of the remainder of this section is to describe and explain various features that can be seen in the movie, such as spiral structures in the spectrum, and the apparent mismatch between stochastic and deterministic dynamics.

The reason we chose to provide more details for the analysis of the stochastic sine circle map over the stochastic integrate-and-fire of Example 2.4 is that its deterministic system has quasiperiodic, periodic, and chaotic regimes. However, our analysis uses general ideas that apply to other situations such as Example 2.4 and its modification, the simplified stochastic integrate-and-fire, in Example 2.3. The movie associated with Fig. 3(B) shows how the spectrum of Π changes with parameter κ in the case of the stochastic integrate-and-fire. See also Sections 4.8 and 4.9.

Our results are more interesting when noise is small, i.e. $\sigma \ll 1$. This is natural, since injecting a large amount of noise causes the Markov chain to mix faster and lose any signs of periodicity or quasiperiodicity. Regions of dominance of different types of dynamics (that we describe below) become blurred and overlapping for larger noise.

We will break our analysis of this example into the different regimes of κ. In the following sections (x_n) will denote the deterministic dynamical system and (X_n) the Markov chain. In our figures we chose to set $a = 0.1$ and $\sigma = 0.05$.

We should note here that the analysis below is for operator Π itself, while the numerical computations performed to plot our figures were done by discretizing operator Π into a 1000×1000 stochastic matrix. We explain in Appendix A how and why this works.

4.1. Below a: $0 < \kappa < a$

In this regime the deterministic map f_κ does not have a fixed point and the sequence (x_n) wraps around the circle $\mathbb{S}$; see Figs. 4(A) and (B) upper. If a is irrational, the deterministic dynamical system is quasiperiodic (i.e. the trajectory densely covers the circle) for a whole interval of κ-values near 0. Outside this interval, or if $a = p_0/q_0$ is rational (as in the parameter in our plots where $a = 1/10$), there are infinitely many intervals of κ-values where the orbit is periodic of period q (see the leftmost part of Fig. 1(A) corresponding to small κ). These intervals are very short: width $w(q)$ of an interval corresponding to period q satisfies $w(q) \sim q^{-\beta}$ with $\beta \approx 2.29$. See [37].

When noise is present in the system, because the intervals with periodic behavior are short and mostly correspond to large periods, periodicity is washed out and the quasiperiodic regime dominates in this range of κ-values. We will say the chain is quasiperiodic. This is confirmed empirically in the numerical simulations, see Fig. 4(B) lower. We next show how the spectrum of transition operator Π may allow us to distinguish this parameter region.

The spectrum of Π consists of two conjugate spirals; see Fig. 4(C). To explain these spirals consider the case $\kappa = 0$. (Recall that Π has countably many eigenvalues accumulating at 0. Thus, only a few are visible in the figure.) For $\sigma > 0$ consider the Markov chain on $\mathbb{S}$ defined by $X_{n+1} = \{X_n + a + \sigma\xi_n\}$, where ξ_n

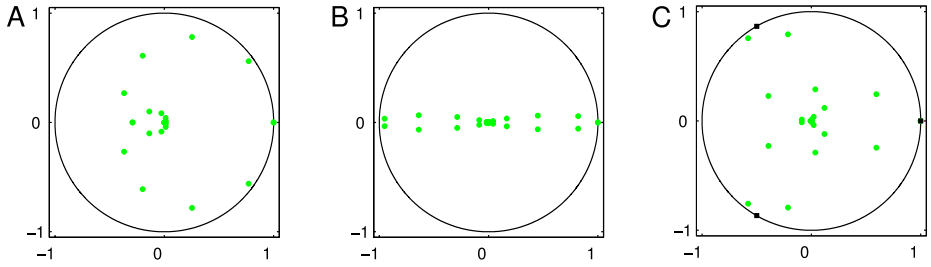

Fig. 5. Plot of the spiral (4.1) with k varying from 0 to 20. (A) $a = 0.1$. (B) $a = 0.505$. (C) $a = 0.354$.

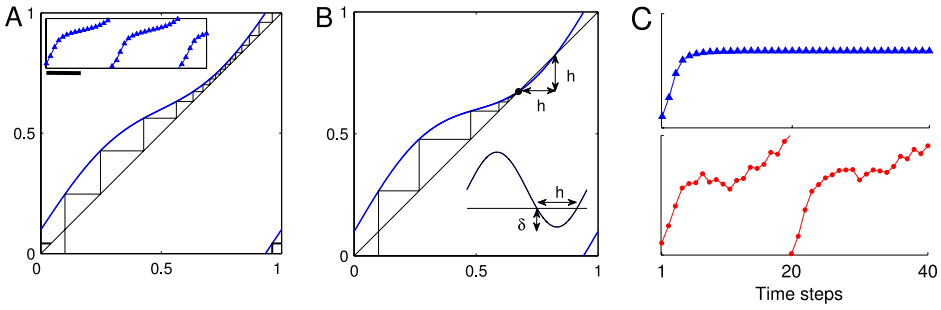

Fig. 6. (A) Sine circle map with $a = 0.1$ and $\kappa = 0.08$, cobwebbing of sequence (x_n) with $x_0 = 0.1$, and the sequence itself, which is still quasiperiodic (inset). The scale bar is 10 time units. (B) Sine circle map with $a = 0.1$ and $\kappa = 0.1125$ and cobwebbing of sequence (x_n) with $x_0 = 0.1$. Here, when $\sigma = 0.05$, $C_1 = 3$ and the trap is still small. Inset shows how the size h of the trap is computed by estimating the distance h between the two solutions of $\sin(2\pi x) = -a/\kappa$ in $(0, 1)$ in terms of the depth $\delta = 1 - a/\kappa$ of the curve. (C) Parameters are $a = 0.1$ and $\kappa = 0.1125$. Upper: Deterministic sequence (x_n) converging monotonically to the fixed point; Lower: Markov chain (X_n) with $\sigma = 0.05$, spending some time near the fixed point, but eventually escaping and still wrapping around $\mathbb{S}$.

is an i.i.d. sequence of standard normal random variables. Then, $\Pi h(x) = E[h(\{x + a + \sigma\xi_1\})]$.

The spectrum of the shift operator $h(x) \mapsto h(\{x+a\})$ is $\{e^{2\pi ika} : k \in \mathbb{Z}\}$, where $i = \sqrt{-1}$. The corresponding eigenfunctions are $\{e^{2\pi ikx} : k \in \mathbb{Z}\}$. So if a is rational, there are finitely many eigenvalues, but they come with infinite multiplicity, since $e^{2\pi ika}$ will match for infinitely many k's.

The spectrum of the heat operator $h(x) \mapsto E[h(\{x + \sigma\xi_1\})]$ is $\{e^{-2\pi^2k^2\sigma^2} : k \in \mathbb{Z}\}$. The corresponding eigenfunctions are again $\{e^{2\pi ikx} : k \in \mathbb{Z}\}$. So 1 has multiplicity 1, but all other eigenvalues have multiplicity 2.

The two operators commute and can be diagonalized simultaneously. As a consequence, the spectrum of the combined operator Π is

$$\{e^{-2\pi^2k^2\sigma^2}e^{2\pi ika} : k \in \mathbb{Z}\} \tag{4.1}$$

and the corresponding eigenfunctions are $\{e^{2\pi ikx} : k \in \mathbb{Z}\}$.

Each eigenvalue has multiplicity 1. The way to visualize the spectrum is to start with the eigenvalue 1 and then every time rotate by an angle of $2\pi a$, both clockwise and counterclockwise, while shrinking the modulus, resulting in a spiral. An example with $a = 0.1$ is shown in Fig. 5(A). This is the exact spectrum for our sine circle map example with $\kappa = 0$. Note that if $2\pi a$ is close to π, then the spectrum looks like two spirals because eigenvalues in (4.1) alternate between having an angle near 0 and an angle near π. Fig. 5(B) shows the spiral for $a = 0.505$. Compare it with early frames of the movie associated with Fig. 3(B) and see also Sections 4.8 and 4.9. Similarly, if $2\pi a$ is close to $2\pi/3$ or $4\pi/3$, the spectrum looks as if it is made out of 3 spirals; see Fig. 5(C).

For small non-zero κ the spectrum will be close to the one for $\kappa = 0$ (Fig. 4(C)). This is because when $\sigma > 0$ operator Π is compact and strongly continuous in κ. Thus, its spectrum is also continuous in κ, in the sense of Lemma A.1 of Appendix A.

The above allows to detect the presence of a spiral, for small κ, by checking if angles are (approximately) equal between consecutive eigenvalues (sorted in decreasing order of their norm).

For larger κ, the angle between consecutive eigenvalues is no longer constant (or close to constant). Adding to this the fact that depending on the value of a, the geometry of spirals (4.1) can be quite complex (Figs. 5(B) and (C)), numerically testing for the presence of a spiral may become a non-trivial task.

In the next two sections we consider the change in stochastic dynamics as the deterministic system undergoes a saddle–node bifurcation. Based on the changes in dynamics and spectrum with κ, as summarized in the movie in Fig. 3, we chose to split the discussion of this regime into two sections: one where the Markov chain can escape the trap made by the saddle–node, and one where the escape becomes highly improbable. We chose to consider that it is still probable for a normally distributed random variable to exceed three standard deviations, while exceeding five standard deviations is highly unlikely. (In probability theory, the former is usually referred to as a central limit, or a small deviation event, while the latter is a large deviation event.) The boundary between the two types of events is in fact vague and the choice of the specific constants 3 and 5 is quite arbitrary. In the following two sections we suggest that the distinction can be made more precise by considering the changes in the spectrum of Π.

4.2. Near a: $a < \kappa < a/(1 - C_1^2\sigma^2\pi^2/2)$ with C_1 small ($C_1 \lesssim 3$)

As κ gets closer to a the corridor which the sequence (x_n) has to cross gets narrower, as Fig. 6(A) shows. The sequence still wraps around $\mathbb{S}$, but spends more time clearing the corridor. When κ goes above a, the corridor vanishes and the sequence (x_n) gets "trapped". The map develops one stable and one unstable fixed points (Figs. 6(B) and (C) upper). (This is the well known saddle–node bifurcation.)

The portion of the map curve below the $y = x$ diagonal, shown in Fig. 6(B), forms a *trap* of height h for the Markov chain as well. The probability the chain clears this trap is $P\{\xi \geq h/\sigma\}$ which is of order $e^{-h^2/(2\sigma^2)}$ (recall that ξ is a standard normal random variable). The time it takes the chain to exit the trap is then of order $e^{h^2/(2\sigma^2)}$.

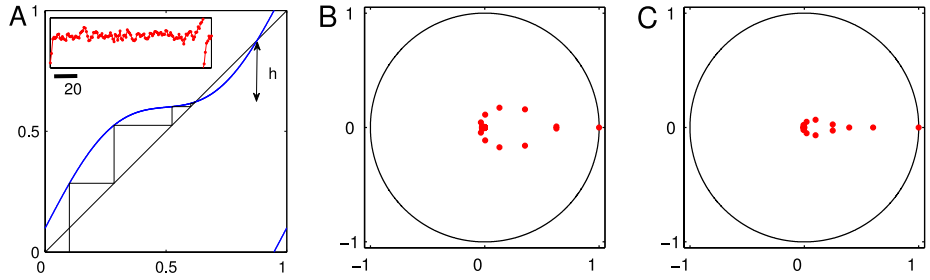

Fig. 7. (A) Sine circle map with $a = 0.1$ and $\kappa = 0.14$ and cobwebbing of (x_n) with $x_0 = 0.1$. Markov chain time course (X_n) with $\sigma = 0.05$ (inset). Here, $C_2 = 4.8$ and the size h of the trap is large. Hence, the chain spends a very long time near the fixed point. Note that the scale bar in this inset is 20 time units. (B) The spectrum of Π at $\kappa = 0.14$ showing the beginning of the "zipping" of the spirals, as the two second-largest eigenvalues collide and become real. (C) The spectrum of Π at $\kappa = 0.167$: the zipping continues, as the fixed point becomes more present.

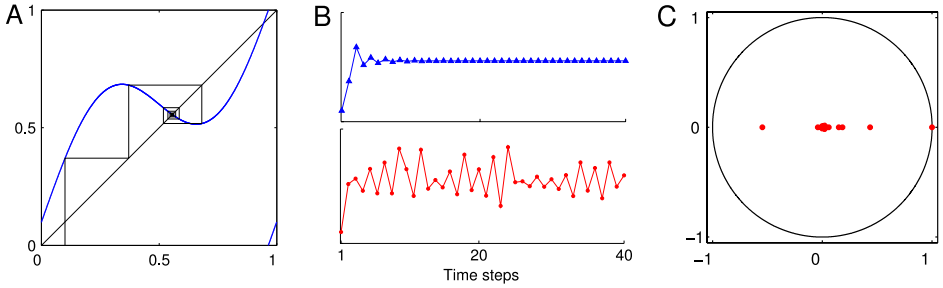

Fig. 8. (A) Sine circle map with $a = 0.1$ and $\kappa = 0.29$ and cobwebbing showing oscillations while converging to the fixed point. (B) Upper: Deterministic sequence (x_n); Lower: Markov chain (X_n) with $\sigma = 0.05$, switching between oscillating around and converging to the fixed point. (C) The spectrum of Π: the negative eigenvalue is now the second largest in modulus.

To compute h we note that it equals the distance between the two solutions of $f_\kappa(x) = x$, which are the same as the solutions of $\sin(2\pi x) = -a/\kappa$ (inset of Fig. 6(B)). When κ is close to a, a Taylor expansion of f_κ near the fixed point shows that $h \approx \sqrt{2(1 - a/\kappa)/\pi^2}$.

When h/σ is small (roughly speaking, the height to clear is less than 3 standard deviations) jumping out of the trap takes a central limit theorem type event to happen, and is hence likely. The Markov chain keeps wrapping around $\mathbb{S}$ and we still consider it quasiperiodic (6(C) lower).

In this regime, the spectrum continues to consist of two conjugate spirals.

4.3. Before $\sqrt{a^2 + 1/(4\pi^2)}$: $a/(1 - C_1^2\sigma^2\pi^2/2) < \kappa$ and $\kappa < a/(1 - C_2^2\sigma^2\pi^2/2)$ with C_2 large ($C_2 \gtrsim 5$)

As the depth h of the trap becomes large it takes a large deviation event for the Markov chain to jump over the trap (i.e. the probability of achieving this becomes extremely small); see Fig. 7(A). The Markov chain spends a long time near the fixed point; see the inset of Fig. 7(A) and note the change of scale on the time-axis. The larger the $C_2 = h/\sigma$ is, the more dominant the periodic regime is.

The above is very well captured by the spectrum. Indeed, the fact that h/σ has become large and the fixed point started to emerge is indicated by the spiral beginning to *zip*. By this, we mean that conjugate eigenvalues "collide" and become real, starting with the two second largest in modulus (Fig. 7(B)). The size of the remaining spiral indicates the amount of contribution of the quasiperiodic regime (Fig. 7(C)).

One can quantify the size of the zipped region as follows: Let λ_k be the eigenvalues of Π ranked so that $1 = \lambda_0 \geq |\lambda_1| \geq \cdots$. Let $K = \min\{k : \lambda_k \in \mathbb{R}, \lambda_{k+1} \notin \mathbb{R}\}$. Then $1 - |\lambda_K|$ indicates the size of the zipped region. We call this quantity the *zipping index*. The right panel in Fig. 11 demonstrates how as the size of the zipped region increases the time it takes the Markov chain to escape the fixed point becomes larger, i.e. stochastic phase locking becomes more pronounced.

4.4. Near $\sqrt{a^2 + 1/(4\pi^2)}$

While κ is below $\sqrt{a^2 + 1/(4\pi^2)}$ the slope at the stable fixed point is positive and (x_n) converges monotonically to the stable fixed point; see Figs. 6(B) and (C) upper, and 7(A). As κ crosses that value the slope switches from positive to negative. At this point the sequence (x_n) starts oscillating around the fixed point as it converges to it; see Figs. 8(A) and (B) upper. The system is starting to prepare for the upcoming cycle of period 2, as explained further in Section 4.5.

Short before $\sqrt{a^2 + 1/(4\pi^2)}$ noise allows the Markov chain more and more to move around the fixed point. A cycle of period 2 starts emerging, although the fixed point regime is still the dominant one. This will happen earlier for larger σ, since the Markov chain has more of a chance to start oscillating around the fixed point. On the spectrum side, the presence of period 2 cycle is manifested by negative eigenvalues becoming nonnegligible. (Remember from Section 3 that for circle map matrices period 2 cycles correspond to eigenvalues of ± 1.) The larger the modulus of the largest negative eigenvalue is, the more present the cycle of period 2 becomes.

Shortly after $\sqrt{a^2 + 1/(4\pi^2)}$, the period 2 cycle starts dominating; see Fig. 8(B) lower. The negative eigenvalue now becomes the second-largest in modulus; see Fig. 8(C).

4.5. Near $\sqrt{a^2 + 1/\pi^2}$

As κ keeps increasing the slope at the fixed point decays towards -1, oscillations take longer, and the fixed point becomes less stable. The second iteration $f_\kappa \circ f_\kappa$ starts going through a similar scenario as the one the first iteration went through. More precisely, as κ gets closer to $\sqrt{a^2 + 1/\pi^2}$ the slope of the second iterate at the fixed point grows closer to 1 and as κ gets larger than this value, its graph crosses the diagonal at three points, the middle one corresponding to an unstable steady state of the map and the other two to a cycle of period 2; see Figs. 9(A) and (B).

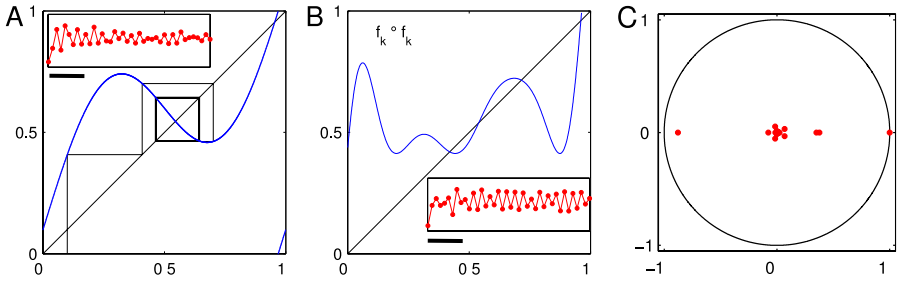

Fig. 9. (A) Sine circle map with $a = 0.1$ and $\kappa = 0.355$, cobwebbing showing a cycle of period 2. Inset: time course of the Markov chain (X_n) with $\sigma = 0.05$ having a dominant period 2 but a still present fixed point regime. Here, the trap in the second iteration $f_\kappa \circ f_\kappa$ is still small. (B) The second iteration of the sine circle map with $a = 0.1$ and $\kappa = 0.405$. The trap is now bigger and the Markov chain spends much more time oscillating between the two fixed points of $f_\kappa \circ f_\kappa$ (inset). Scale bar on both insets is 10 time units. (C) The spectrum of Π at $\kappa = 0.405$: the second-largest eigenvalue is very close to -1.

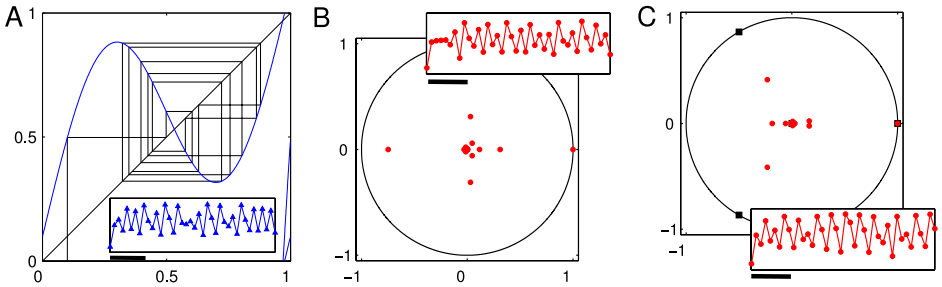

Fig. 10. (A) Sine circle map with $a = 0.1$ and $\kappa = 0.509$ and both cobwebbing and sequence (x_n) showing chaos. (B) The spectrum of Π at $\kappa = 0.462$ with the largest eigenvalues aligned at right angles. The inset shows the Markov chain having cycle of period 4 emerges. (C) The spectrum of Π at $\kappa = 0.53$ with the largest eigenvalues aligned at $2\pi/3$ angle; the small squares on the unit circle mark the third roots of 1. The inset shows the Markov chain having a cycle of period 3 emerges. Marked scale on all insets is 10 time units.

In the stochastic system, however, the presence of a cycle of period 2 becomes very strong but the stable fixed point is still felt. More precisely, the Markov chain oscillates for a long time around the fixed point, but then approaches the fixed point for another long period of time. This behavior is similar to what happened near $\kappa = a$: the second iteration $f_\kappa \circ f_\kappa$ does not yet present a large trap; see the inset of Fig. 9(A). After that, the trap gets larger and excursions that stay close to the fixed point become more rare; see Fig. 9(B).

This is again captured by looking at the spectrum: as the trap gets larger, the negative eigenvalue gets closer to -1. The fixed point regime starts becoming negligible when this eigenvalue is at its closest to -1; see Fig. 9(B). The Markov chain can now be considered periodic of period 2.

To quantify the strength of the different periodic scales introduce the function

$$R(\xi) = \left|\sum_{k=0}^{\infty} r_k e^{2\pi i \xi \varphi_k}\right|, \tag{4.2}$$

where $r_k e^{2\pi i \varphi_k}$ are the eigenvalues of Π. The magnitude of $R(p)$ corresponds to the relative dominance of q:p phase-locking in the stochastic dynamics. The left panel in Fig. 11 demonstrates how certain scales are more dominant than others, as κ varies.

On a related note, it was shown in Section 2 of [15] that under some technical conditions on the underlying deterministic system (in particular, periodicity) and in the limit $\sigma \to 0$, the second largest eigenvalue of Π converges to -1 in the period two case, while in the period four case the top four eigenvalues converge to the fourth roots of 1, etc. Although, these results support our observations in the above two sections, they do not directly apply as we consider the case of a fixed $\sigma > 0$.

4.6. Larger κ

The above process continues as the deterministic system develops cycles of period 4, then 8, then 16, and so on; see Fig. 1(A). At a finite κ, the length of the cycle reaches infinity. In contrast to the quasiperiodic case, map f_κ is not orientation preserving and the sequence (x_n) is "out of order" and is thus very sensitive to initial conditions. The deterministic system is said to have become *chaotic*. See Fig. 10(A).This is the period-doubling route to chaos. Notice that in our case the range of the map is quite limited (Fig. 1(A)) and thus the trajectory often goes through sequences of similar, but not repeating values.

This scenario repeats again and again, with cascades of period doublings starting at all possible odd periods p and leading eventually to chaos. Very small changes in the parameter in this regime can tune the system into periodic or chaotic dynamics.

The process also continues in the stochastic case, with the emergence of a cycle of period 4 that starts becoming more and more dominant; see the inset of Fig. 10(B). On the spectrum side 2 purely imaginary eigenvalues emerge indicating that a cycle of period 4 is becoming more present (as explained in Section 3). These eigenvalues grow in modulus, indicating that the cycle of period 4 is becoming more dominant; see Fig. 10(B).

As we have shown before for the fixed point and period 2 regimes, in the stochastic system the change of dynamics starts at earlier values of the parameter than for the deterministic system (i.e. cycles emerge earlier). It also lasts longer (cycles stay dominant for longer). Thus noise, in a sense, perturbs the parameter κ, and when the deterministic system becomes sensitive to changes in κ, e.g. when cascades become too short, close to and during the chaotic phase as explained above for the deterministic system, certain periods (including the chaotic regime) may never get a chance to become dominant, while certain other periods may dominate. Which periods dominate now depends very delicately on the interplay between the parameter κ and noise strength σ, and the motion of the eigenvalues thus seems less organized. Furthermore, at some values of κ several dynamic regimes compete, and the Markov chain looks more ergodic than when one regime is dominant.

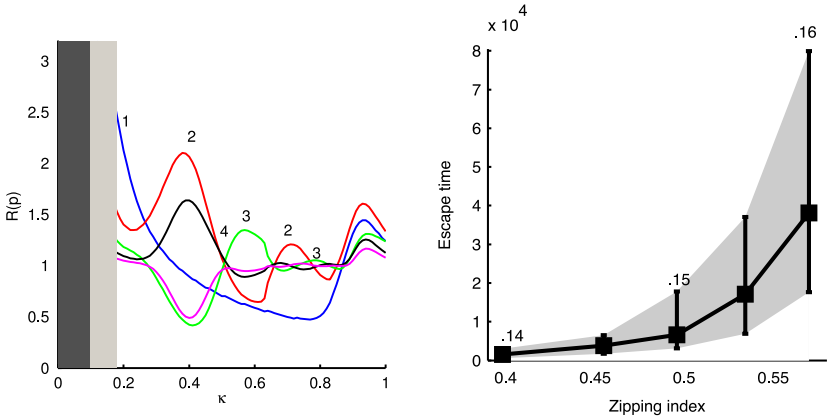

Fig. 11. Left: Summary of the analysis of stochastic sine circle map with $a = 0.1$ and $\sigma = 0.05$. The numbers above the graphs indicate the dominant period. Right: Zipping index vs. median escape time. The error bars give the first and third quartiles. Values of parameter κ are indicated above the error bars.

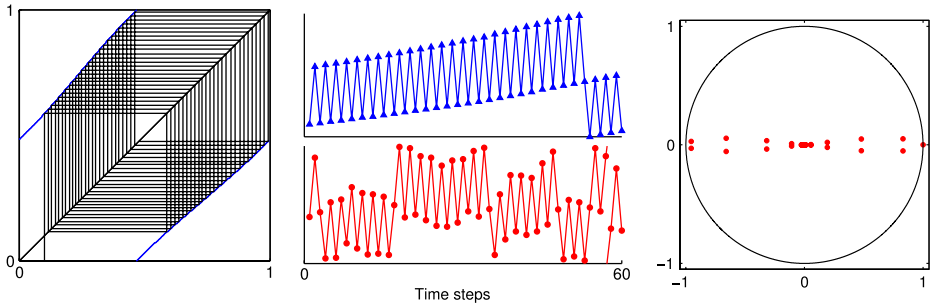

Fig. 12. Left: Integrate-and-fire with $\tau = 2$, $I = 0.7$, $\kappa = 0.045$, and the first few steps of cobwebbing of the deterministic sequence with starting point 0.1. Upper center: Deterministic sequence; Lower center: Markov chain (T_n) with $\sigma = 0.01$. Both sequences are wrapping densely around $\mathbb{S}$ and are hence quasiperiodic. Right: The spectrum of Π exhibiting the spirals.

In the particular example we are considering, when the noise is not too small ($\sigma = 0.05$), the whole region in the Feigenbaum diagram between the period 4 and period 3 regimes of the deterministic system (κ between about 0.45 and 0.55 in Fig. 1(A)) is smoothed out, and the Markov chain simply transitions from having a more dominant period 4 regime to a more dominant period 3 regime (Figs. 10(B) and (C)).

Note that in our example, when $a = 0.1$ and κ goes above 0.9 a long enough interval of period doubling occurs; see Fig. 1(A). Then the above stochastic bifurcation scenarios (described in Sections 4.1 through 4.6) are clearly observed again.

4.7. Summary

The left panel in Fig. 11 summarizes our analysis of the stochastic sine circle map. The dark gray shaded region represents the quasiperiodic regime. The light gray region corresponds to zipping where the dynamics are transitioning from quasiperiodic to phase-locked. The curves are the graphs of $R(p)$, $1 \le p \le 5$, as functions of κ. We see that right after zipping ends the system is phase-locked with period 1. This is followed by a period 2 phase-locking, then period 4, then 3, then 2, then 3 again. After that, several periodic regimes compete at the same time and the Markov chain becomes chaotic.

The right panel of the figure demonstrates the increasing correspondence between the zipping index (the size of the zipped region) and the escape time of the Markov chain from the fixed point.

4.8. The stochastic integrate-and-fire model

Our analysis works for other diffusion processes with a constant diffusion coefficient σ^2. If the diffusion coefficient is not constant (e.g. in the case of multiplicative noise), a random time change brings the situation back to one with constant σ and our analysis applies again.

As an example, we summarize the results in the case of the stochastic integrate-and-fire model from Example 2.4. In this case, transition density $p(y|x)$ satisfies an integral equation that we solve numerically using the method described in [32]. The movie associated with Fig. 3(B) shows how the spectrum and the dynamics of this model change with parameter κ. The relationship between the spectrum and dynamics follows the same principles as described for the sine map, thus we will only comment here on selected regimes and transitions.

First, for κ small, the spectrum represents a spiral. Visually, it is not readily apparent (Fig. 12, Right). Let us compute the parameters of the spiral. For $\kappa = 0$ we can compute the map, starting from $T_n = 0$. It is equal to $T_{n+1} = -\tau \log(1 - 1/(\tau I)) = 0.505$. Setting the spiral parameter a to 0.505 we obtain the spiral shown in Fig. 5(C), which approximates the one for small κ very closely (Fig. 12, Right). Dynamics of the Markov chain are thus quasiperiodic. Notice that in this example (as in its deterministic counterpart) the values oscillate as they wrap around $\mathbb{S}$ in the quasiperiodic regime.

Near $\kappa = 0.08$ zipping of the spiral begins. Note that here the zipping starts from the left side, since that is where the second-largest eigenvalues are. Consequently, a cycle of period 2 emerges. However, escaping it takes a central limit event and the Markov chain is still quasiperiodic. See the middle panel in Fig. 13. As κ grows the period 2 cycle becomes more dominant. Near $\kappa = 0.24$ zipping is complete and the Markov chain is phase-locked with period 2: escaping the period 2 cycle takes a large deviation event. See the right panel in Fig. 13.

At $\kappa = 0.544$ period 5 dominates in the stochastic model; see Fig. 14. The value of κ is taken from the intersection of the curves

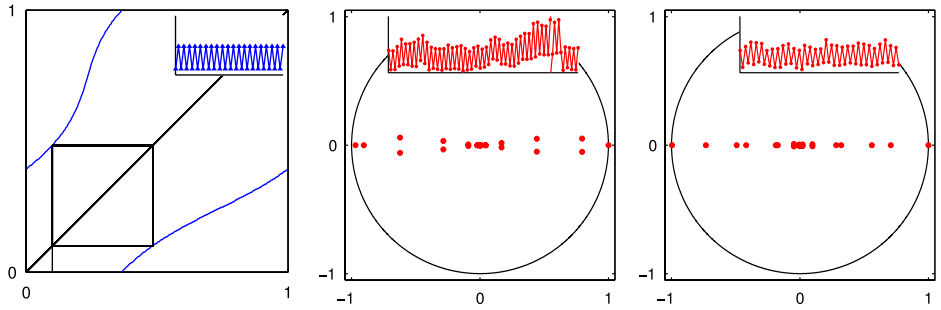

Fig. 13. Left: Integrate-and-fire with $\tau = 2$, $I = 0.7$, $\kappa = 0.13$, and the first few steps of cobwebbing of the deterministic sequence with starting point 0.1; The inset shows the deterministic sequence showing a cycle of period 2. Center: The spectrum of Π with $\kappa = 0.13$ and $\sigma = 0.01$ exhibiting zipping; The inset shows how the Markov chain (T_n) oscillates near the periodic cycle for a long time, then escapes and wraps around $\mathbb{S}$. Right: The spectrum of Π with $\kappa = 0.24$ and $\sigma = 0.01$ indicating a period 2 cycle; The inset shows the Markov chain (T_n).

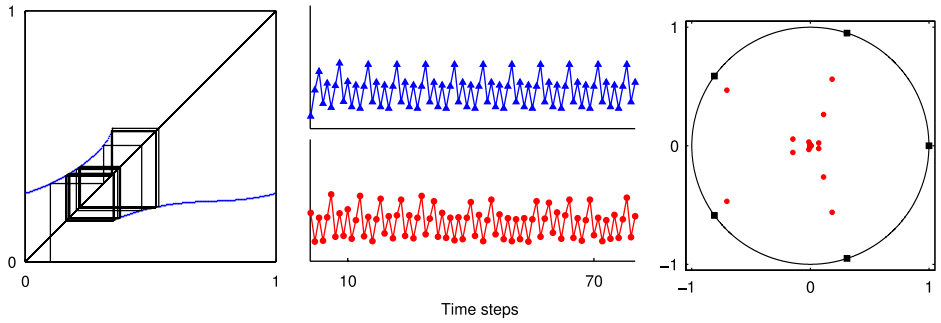

Fig. 14. Left: Integrate-and-fire with $\tau = 2$, $I = 0.7$, $\kappa = 0.59$, and the first few steps of cobwebbing of the deterministic sequence with starting point 0.1. Upper center: Deterministic sequence showing a cycle of period 7; Lower center: Markov chain (T_n) with $\sigma = 0.01$. Right: The spectrum of Π exhibiting a cycle of period 5; the small squares on the unit circle mark the fifth roots of 1.

$R(1)$ and $R(5)$; see the left panel in Fig. 15. In the deterministic model, the system has a cycle of period 7 at this value of κ. See Figs. 14 and 1 (A).

At this range of κ the deterministic dynamical regimes are too short to fully develop in the stochastic case. The period 5 cycle transitions to a period 3 cycle which starts dominating at $\kappa = 0.635$ (intersection of $R(5)$ and $R(3)$ in Fig. 15, Left). For larger κ similar transitions occur. E.g. at $\kappa = 0.839$ period 4 becomes dominant, etc. See the movie associated with Fig. 3(B).

The left panel of Fig. 15 summarizes the above analysis. The right panel demonstrates how the size of the zipped region is again in an increasing relationship with the escape time of the Markov chain from the periodic cycle.

4.9. The simplified stochastic integrate-and-fire model

The same analysis can be repeated in the case of the simplified stochastic integrate-and-fire model from Example 2.3. However, as was mentioned after Example 2.4, it is shown in [14] that for small values of σ, the simplified stochastic integrate-and-fire process is very close to the process in Example 2.4 with a different but also small σ. Thus, the results of the analysis of the two models are very similar. We therefore only give the summary of the analysis for this model in Fig. 16.

5. Discussion

We have demonstrated that the dynamics of a finite state dynamical system as well as those of certain Markov chains on the circle can be related to specific properties of the spectrum of the associated transition operator. Namely, we have demonstrated that for finite state dynamical systems the eigenvalues of the transition matrix reveal the cycle lengths and the eigenvectors show the attractors along with their transients. More importantly, we have also shown that for a class of Markov chains on the circle, quasiperiodicity in the dynamics can be seen by observing spiral structures in the spectrum of the transition operator, and that dominance of quasiperiodicity and the different phase-locked regimes can be understood in terms of "zipping" of the spectrum and emergence of eigenvalues approximating scaled roots of 1, respectively. The spiral structures were also observed when Gaussian noise was replaced by a uniform noise over a small interval, or a bimodal combination of two Gaussian noises. Thus, we believe these structures to occur more generally, e.g. when the noise is concentrated in a small region, relative to the size of the circle. The precise mathematical reason behind the spirals remains an interesting open question.

The spectral approach presented here is likely to be productive in many different contexts. For example, it can be used to predict dynamical regimes of computational models without direct simulation. Note that even though our examples have been one-dimensional, our approach can be applicable to more complex models, that can be projected to a suitable one-dimensional manifold, e.g. phase-oscillators. In the context of experimental studies, such as recordings of spiking neurons in the presence of noise, it can be used to categorize the recorded spiking as quasiperiodic, or having a particular mode of phase-locking.

Additionally, our results suggest a new definition of a periodic and quasiperiodic Markov chain, based on the shape of its spectrum. Moreover, our results also suggest a new notion of stochastic bifurcation, based on changes in the spectrum of the transition operator. It is important to note that we have distinguished parameter ranges when the new dynamical regime "emerges" and then when it becomes "dominant". Thus, we are suggesting that "stochastic bifurcation points" should rather be thought of as "cascades" or "stochastic bifurcation regions".

As we mentioned in Section 2.3, one of the accepted notions of stochastic bifurcation is "P-bifurcation", in which the shape of

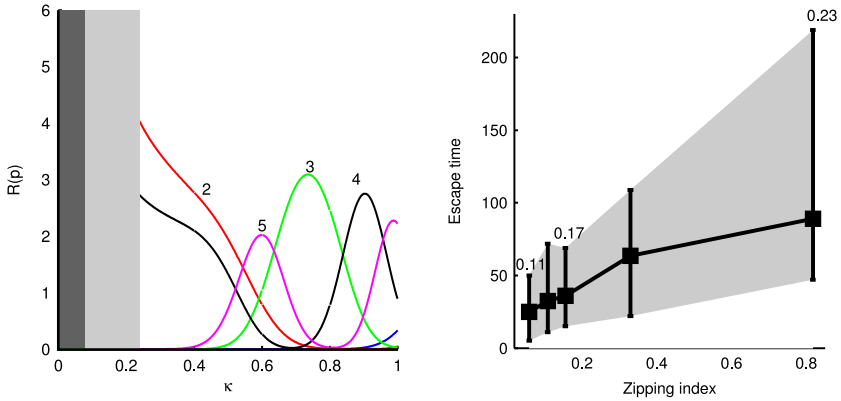

Fig. 15. Left: Summary of the analysis for stochastic integrate-and-fire with $I = 0.7$, $\tau = 2$, and $\sigma = 0.01$. The numbers above the graphs indicate the dominant period. Right: Zipping index vs. median escape time. The error bars give the first and third quartiles. Values of parameter κ are indicated above the error bars.

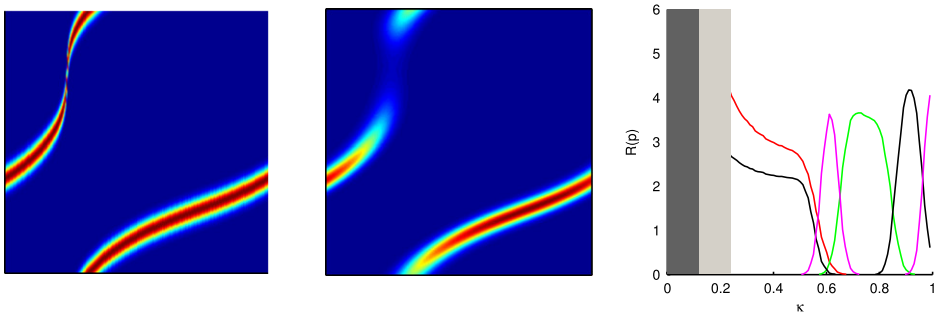

Fig. 16. Left: Density of operator Π corresponding to the simplified stochastic integrate-and-fire with $I = 0.7, \tau = 2, \sigma = 0.03$, and $\kappa = 0.19$. Center: Density of operator Π corresponding to the stochastic integrate-and-fire with $I = 0.7, \tau = 2, \sigma = 0.01$, and $\kappa = 0.19$. Right: Summary of the analysis for the simplified stochastic integrate-and-fire with $I = 0.7, \tau = 2$, and $\sigma = 0.01$.

the invariant measure density undergoes qualitative changes. This notion is closely linked to the work in this paper, as the invariant measure density is the eigenfunction of Π, corresponding to eigenvalue 1. Indeed, we see peaks of the eigenfunction developing and disappearing at various parameter values (video associated with Fig. 3(A)), but the most dominant regime cannot always be read from them. For example, in the case of the stochastic sine circle map at $a = 0.1, \kappa = 0.32$, and $\sigma = 0.05$, a period 2 cycle dominates as can be observed from the eigenvalues and from the trajectory. However, the invariant measure density only has one peak, as the center between two preferred locations will be visited (due to randomness) on the way either up or down, and thus overall visited more frequently than either location. Perhaps, it is not surprising that the invariant measure density does not capture the essential features of the dynamics, as one eigenfunction only carries part of the information, while looking at the whole spectrum gives more.

Other ways of describing qualitative changes in stochastic dynamics have been employed, such as D-bifurcations [34] and reliability [35,31,38]. Relating our spectral approach to this existing body of work will be the subject of future investigations.

The method presented in this paper critically relies on the knowledge of the transition probability $p(y|x)$ of the given process. The examples we used had the advantage that this probability was easily computable. In many other situations, given a model in terms of stochastic differential equations, one would need to rely on numerical methods to solve an integral equation for $p(y|x)$. Such numerical methods have been derived for Ornstein–Uhlenbeck processes, which includes cases of the stochastic integrate-and-fire model; see [32]. Developing such methods for the more complex, e.g. multidimensional, situations is essential and is another future project.

Moreover, in the cases where the method can be applied to experimental studies, its feasibility will depend on the size of discretization N, as more data will be required to estimate transition probabilities for larger N. In our examples we have used $N = 1000$ since it was not numerically expensive to do so. However, we have observed that even $N = 100$ is sufficient to predict the dynamics. Nevertheless, sensitivity to N is likely to vary from model to model and is also left for a future investigation.

The work presented in this manuscript has been partially motivated by recent work on the phase-locking of periodically-driven neurons in the presence of noise [39]. In neuroscience, a common measure of phase-locking in a noisy system is the so-called *vector strength*. Our results suggest that dominance of the appropriate dynamic regime (such as the size of the spiral in the quasiperiodicity to phase-locking transition or function R from (4.2) in the phase-locked regimes) may serve as an alternative.

One situation in which the stochastic spike phase return maps can be computed is when the stimulus is a periodic train of brief pulses, the neuron has a well-defined deterministic phase response curve (PRC), and the variability of the phase response in the presence of noise can be evaluated as well. Such stochastic PRCs have been computed in experiments [40] and their variance has also been analytically derived under conditions of small noise and weak stimulus [41]. Once the PRC is computed, the stochastic spike phase return map can also be obtained [42]. As intrinsic properties of the oscillators change (e.g. in experiment or through mutations), it will affect their PRCs, which will in turn modify the ability of the cell to entrain to external input (as can be quantified by the spectral methods we presented).

In conclusion, we have presented a promising approach for classifying the dynamics of stochastic circle maps based on the geometry of the spectra of the associated transition operators. The results presented in this article motivate further development of

a mathematically rigorous theory and exploration in a variety of applications.

Acknowledgments

Alla Borisyuk was supported in part by NSF grant DMS-1022945. Firas Rassoul-Agha was supported in part by NSF grant DMS-0747758.

Appendix A. Discretization of the transition operator

Recall the transition operator Π of the Markov chain, defined in (2.1). We will assume the following throughout the appendix.

Hypothesis A.1. Transition operator Π has a transition density (or kernel) $p(y|x)$ relative to Lebesgue measure; i.e. $\Pi h(x) = \int_0^1 p(y|x)h(y)\,dy$. Furthermore, $p(y|x)$ is bounded in x and y and continuous in y uniformly over x:

$$\lim_{\delta\to 0}\sup\{|p(y|x)-p(y'|x)| : x,y,y'\in\mathbb{S}, \quad |y-y'|<\delta\} = 0. \tag{A.1}$$

$p(y|x)$ is also continuous in x uniformly over y except for, possibly, finitely many x-values; i.e. $\exists \hat{x}_1,\dots,\hat{x}_m \in \mathbb{S}$ (which could be empty, and then $m=0$) such that

$$\lim_{\delta\to 0}\sup\{|p(y|x)-p(y|x')| : x,x',y\in\mathbb{S}, |x-x'|<\delta, \quad |x-\hat{x}_k|>\delta, |x'-\hat{x}_k|>\delta, \forall k=1,\dots,m\} = 0. \tag{A.2}$$

This hypothesis is clearly satisfied in the case of Example 2.3 when F has finitely many discontinuities in $[0,1]$ and ξ_1 has a continuous density relative to Lebesgue measure. It is also satisfied for a wide class of diffusion processes, such as ones with smooth diffusion and drift coefficients, in which case $p(y|x)$ is continuous in both x and y; see [43]. This includes Example 2.4. On the other hand, Hypothesis A.1 is not satisfied in the case of deterministic dynamical systems, i.e. when $\Pi h(x) = h(f(x))$ for some $f:\mathbb{S}\to\mathbb{S}$.

Compactness of $\mathbb{S}$ and the above hypothesis, in particular (A.1), imply that Π is a compact operator; see Example 4.1 of Chapter 3 of [36].

We would like to approximate operator Π, satisfying the Hypothesis A.1, by a sequence of matrices in a way that the spectra of the matrices "converge" to that of Π.

Fix an integer $N \geq 1$ (the *resolution* of the discretization) and define

$$\pi^N_{i,j} = \frac{p\left(\frac{j}{N}|\frac{i}{N}\right)}{\sum_{k=1}^N p\left(\frac{k}{N}|\frac{i}{N}\right)}, \quad 1\leq i,j\leq N, \quad \text{and}$$

$$\Pi_N h(x) = \sum_{i,j=1}^N \pi^N_{i,j} h\left(\tfrac{j}{N}\right)\mathbb{1}_{\left(\frac{i-1}{N},\frac{i}{N}\right]}(x),$$

for a continuous bounded function $h:\mathbb{S}\to\mathbb{R}$. Then

$$\begin{aligned}
&|(\Pi_N-\Pi)h(x)| \\
&\leq \left|\sum_{i,j=1}^N\Big(\Big[\sum_{k=1}^N p\left(\tfrac{k}{N}|\tfrac{i}{N}\right)\Big]^{-1} - N^{-1}\Big)p\left(\tfrac{j}{N}|\tfrac{i}{N}\right) \right. \\
&\qquad \left. \times h(\tfrac{j}{N})\mathbb{1}_{\left(\frac{i-1}{N},\frac{i}{N}\right]}(x)\right| \\
&\quad + \left|\sum_{i,j=1}^N N^{-1}\left(p\left(\tfrac{j}{N}|\tfrac{i}{N}\right) - p\left(\tfrac{j}{N}|x\right)\right)h\left(\tfrac{j}{N}\right)\mathbb{1}_{\left(\frac{i-1}{N},\frac{i}{N}\right]}(x)\right| \\
&\quad + \left|\sum_{j=1}^N h\left(\tfrac{j}{N}\right)\int_{(j-1)/N}^{j/N}\left(p\left(\tfrac{j}{N}|x\right) - p(y|x)\right)\,dy\right| \\
&\quad + \left|\sum_{j=1}^N \int_{(j-1)/N}^{j/N}\left(h\left(\tfrac{j}{N}\right) - h(y)\right)\,p(y|x)\,dy\right| \\
&\leq \sup_{y\in\mathbb{S}}|h(y)|\max_{1\leq i\leq N}\left|N^{-1}\sum_{k=1}^N p\left(\tfrac{k}{N}|\tfrac{i}{N}\right) - 1\right| && \text{(A.3)} \\
&\quad + \sup_{y\in\mathbb{S}}|h(y)|\sum_{i=1}^N \max_{1\leq j\leq N}\left|p\left(\tfrac{j}{N}|\tfrac{i}{N}\right)\right. \\
&\quad \left. - p\left(\tfrac{j}{N}|x\right)\right|\mathbb{1}_{\left(\frac{i-1}{N},\frac{i}{N}\right]}(x) && \text{(A.4)} \\
&\quad + \sup_{y\in\mathbb{S}}|h(y)|\sup\{|p(y'|x)-p(y|x)| : \\
&\quad x,y,y'\in\mathbb{S}, |y-y'|<1/N\} && \text{(A.5)} \\
&\quad + \sup\{|h(y')-h(y)| : y,y'\in\mathbb{S}, |y-y'|<1/N\}. && \text{(A.6)}
\end{aligned}$$

By continuity of h on the compact set $\mathbb{S}$ the term on line (A.6) converges to 0 as $N\to\infty$. The term on line (A.3) can be bounded by

$$\begin{aligned}
&\sup_{y\in\mathbb{S}}|h(y)|\max_{1\leq i\leq N}\left|N^{-1}\sum_{k=1}^N p\left(\tfrac{k}{N}|\tfrac{i}{N}\right) - 1\right| \\
&\leq \sup_{y\in\mathbb{S}}|h(y)|\max_{1\leq i\leq N}\sum_{k=1}^N\int_{(k-1)/N}^{k/N}\left|p\left(\tfrac{k}{N}|\tfrac{i}{N}\right) - p\left(y|\tfrac{i}{N}\right)\right|\,dy \\
&\leq \sup_{y\in\mathbb{S}}|h(y)|\sup\{|p(y'|x)-p(y|x)| : \\
&\quad x,y,y'\in\mathbb{S}, |y-y'|<1/N\}
\end{aligned}$$

which equals the term on line (A.5) which in turn converges to 0 as $N\to\infty$ due to (A.1). Lastly, the term on line (A.4) is bounded above by

$$\begin{aligned}
&\sup_{y\in\mathbb{S}}|h(y)|\sum_{i=1}^N\max_{1\leq j\leq N}\left|p\left(\tfrac{j}{N}|\tfrac{i}{N}\right) - p\left(\tfrac{j}{N}|x\right)\right|\mathbb{1}_{\left(\frac{i-1}{N},\frac{i}{N}\right]}(x) \\
&\leq \sup_{y\in\mathbb{S}}|h(y)|\sup\{|p(y|x)-p(y|x')| : \\
&\quad x,x',y\in\mathbb{S}, |x-x'|<1/N, \\
&\quad |x-\hat{x}_k|>1/N, |x'-\hat{x}_k|>1/N, \forall k=1,\dots,m\} \\
&\quad + 2\sup_{y\in\mathbb{S}}|h(y)|\sup_{y,z\in\mathbb{S}}p(y|z)\sum_{k=1}^m\mathbb{1}_{\left(\hat{x}_k-\frac{2}{N},\hat{x}_k+\frac{2}{N}\right)}(x).
\end{aligned}$$

Then, by (A.2) the above goes to 0 as $N\to\infty$ for all $x\notin\{\hat{x}_1,\dots,\hat{x}_m\}$. (Recall that $\hat{x}_1,\dots,\hat{x}_m$ are the possible discontinuities of $p(y|x)$ as stated in Hypothesis A.1.)

We have thus shown that $\|\Pi_N-\Pi\|\to 0$ and the sequence of operators Π_N converges to Π in the generalized sense; see Theorem 2.23 of Chapter 4 of [36]. Since the action of the transition operator Π on bounded continuous functions completely determines the distribution of the corresponding Markov chain, we see that this Markov chain can be recovered from operators Π_N. We are particularly interested in recovering the spectrum of Π.

Note that Π_N is a finite rank operator with the range being the linear span of the functions $\mathbb{1}_{[i/N,(i+1)/N)}(x)$. Hence, it has a finite spectrum. The eigenvalues of Π_N are the same as those of the matrix $(\pi^N_{i,j})_{i,j}$ and if $v=(v_0,\dots,v_{N-1})$ is an eigenvector of this matrix, then $\sum_{i=0}^{N-1}v_i\mathbb{1}_{[i/N,(i+1)/N)}$ is an eigenfunction of Π_N. In other words, Π_N can really be viewed as a stochastic matrix, which in turn is completely determined by its eigenvalues and eigenspaces.

Then, the fact that Π_N converges to Π reproves that Π is a compact operator. Thus, Π has a discrete spectrum with countably many nonzero eigenvalues of finite multiplicities, possibly accumulating at 0.

Next, observe that for any $\varepsilon > 0$ there exists an $N_0 > 0$ such that $N \geq N_0$ implies that

$$\sup_{\lambda \in \sigma(\Pi^N)} d(\lambda, \sigma(\Pi)) < \varepsilon;$$

see Remark 3.3 of Chapter 4 of [36]. ($d(\lambda, \sigma(\Pi))$ denotes the Euclidean distance in the space of complex numbers of the point λ to the spectrum of Π.) Moreover, if $\lambda_1, \ldots, \lambda_k \in \sigma(\Pi)$ are separated from the rest of $\sigma(\Pi)$ by a closed curve Γ, then for N large enough the total multiplicity of $\sigma(\Pi^N)$ inside Γ is equal to the total multiplicity of $\lambda_1, \ldots, \lambda_k$; see Section 3.5 of Chapter 4 of [36]. In fact, if $\lambda \in \sigma(\Pi) \setminus \{0\}$, then it can be separated by a closed curve Γ from the rest of $\sigma(\Pi)$ and thus for N large enough Π_N has only one eigenvalue λ_N inside Γ, with the same multiplicity as λ, and the projection operator onto eigenspace $\mathscr{E}_{\lambda_N}(\Pi_N)$ converges in norm to the projection onto $\mathscr{E}_\lambda(\Pi)$, as $N \to \infty$; see Theorem 3.16 of Chapter 4, (6.19) of Chapter 3, and (5.22) of Chapter 1 in [36]. (Note that the uniqueness of the spectral representation of a finite rank operator means that the statements of this paragraph are valid for both geometric and algebraic eigenspaces; see Section 5.4 of Chapter 1 of [36].) We thus have the following lemma.

Lemma A.1. *Assume Hypothesis A.1 holds. Then, away from 0, the spectra and corresponding eigenspaces of the operators Π^N (and hence also the matrices π^N) converge to those of Π, in the sense of the above paragraph.*

This lemma says that one can approximate the spectrum and eigenfunctions of Π by those of the matrix π^N.

Our choice to discretize the operator Π is not the only way to go. In fact any discretization for which Lemma A.1 holds works. For example, the following also works:

$$\pi^N_{i,j} = N \int_{i/N}^{(i+1)/N} \int_{j/N}^{(j+1)/N} p(y|x)\, dx\, dy, \quad \text{and}$$

$$\Pi_N h(x) = N \sum_{i=0}^{N-1} \Big[\sum_{j=0}^{N-1} \pi^N_{i,j} \int_{j/N}^{(j+1)/N} h(y)\, dy \Big] \mathbb{1}_{[i/N,(i+1)/N)}(x).$$

Remark A.2. Note that the above discussion was for a fixed $\sigma > 0$, which is the situation considered in this article. When $\sigma = 0$, i.e. in the case of a deterministic dynamical system, the discretization may fail in approximating the spectrum; see [44] for situations where this happens and [45] for situations where the discretization succeeds. Consequently, as σ gets smaller the discretization may get worse, i.e. N may have to be chosen larger to achieve the same prescribed error size. One way to estimate how large N needs to be (to approximate finitely many eigenvalues of Π) comes by using bounds (A.3)–(A.6) to estimate $\|\Pi_N - \Pi\|$. For instance, in Example 2.3 one has a crude uniform upper bound of C/σ^3 on the x- and y-derivatives of $p(y|x)$. This leads to the estimate

$$\|\Pi_N - \Pi\| \leq C/(\sigma^3 N).$$

Appendix B. Supplementary data

Supplementary material related to this article can be found online at http://dx.doi.org/10.1016/j.physd.2014.07.006.

References

[1] R.L. Devaney, An Introduction to Chaotic Dynamical Systems, second ed., in: Addison-Wesley Studies in Nonlinearity, Addison-Wesley Publishing Company Advanced Book Program, Redwood City, CA, 1989.
[2] P. Collet, J.-P. Eckmann, Iterated Maps on the Interval as Dynamical Systems, in: Progress in Physics, vol. 1, Birkhäuser, Boston, Mass., 1980.
[3] L. Glass, Cardiac arrhythmias and circle maps—a classical problem, Chaos 1 (1) (1991) 13–19.
[4] B. Adamczewski, D. Damanik, Linearly recurrent circle map subshifts and an application to Schrödinger operators, Ann. Henri Poincaré 3 (5) (2002) 1019–1047.
[5] J.P. Keener, F.C. Hoppensteadt, J. Rinzel, Integrate-and-fire models of nerve membrane response to oscillatory input, SIAM J. Appl. Math. 41 (3) (1981) 503–517.
[6] S. Coombes, Liapunov exponents and mode-locked solutions for integrate-and-fire dynamical systems, Phys. Lett. A 255 (2) (1999) 49–57.
[7] S. Coombes, P.C. Bressloff, Mode locking and Arnold tongues in integrate-and-fire neural oscillators, Phys. Rev. E (3) 60 (2, part B) (1999) 2086–2096.
[8] E.A. Coddington, N. Levinson, Theory of Ordinary Differential Equations, McGraw-Hill Book Company, Inc., New York, Toronto, London, 1955.
[9] J. Guckenheimer, P. Holmes, Nonlinear Oscillations, Dynamical Systems, and Bifurcations of Vector Fields, in: Applied Mathematical Sciences, vol. 42, Springer-Verlag, New York, 1983.
[10] S. Strogatz, Nonlinear Dynamics and Chaos: with Applications To Physics, Biology, Chemistry, and Engineering, first ed., in: Studies in Nonlinearity, Westview Press, 2001.
[11] A. Lasota, M.C. Mackey, Chaos, Fractals, and Noise: Stochastic Aspects of Dynamics, second ed., in: Applied Mathematical Sciences, vol. 97, Springer-Verlag, New York, 1994.
[12] R. Rudnicki, K. Pichór, M. Tyran-Kamińska, Markov semigroups and their applications, in: P. Garbaczewski, R. Olkiewicz (Eds.), Dynamics of Dissipation, in: Lecture Notes in Physics, vol. 597, Springer, Berlin, Heidelberg, 2002, pp. 215–238.
[13] V. Baladi, Positive Transfer Operators and Decay of Correlations, in: Advanced Series in Nonlinear Dynamics, vol. 16, World Scientific Publishing Co. Inc., River Edge, NJ, 2000.
[14] P. Baxendale, J. Mayberry, A spectral analysis of the sequence of firing phases in stochastic integrate-and-fire oscillators, Preprint.
[15] J. Mayberry, Gaussian perturbations of circle maps: a spectral approach, Ann. Appl. Probab. 19 (3) (2009) 1143–1171.
[16] T. Tateno, S. Doi, S. Sato, L.M. Ricciardi, Stochastic phase lockings in a relaxation oscillator forced by a periodic input with additive noise: A first-passage-time approach, J. Stat. Phys. 78 (1995) 917–935.
[17] T. Shimokawa, K. Pakdaman, T. Takahata, S. Tanabe, S. Sato, A first-passage-time analysis of the periodically forced noisy leaky integrate-and-fire model, Biol. Cybernet. 83 (2000) 327–340.
[18] T. Tateno, Y. Jimbo, Stochastic mode-locking for a noisy integrate-and-fire oscillator, Phys. Lett. A 271 (4) (2000) 227–236.
[19] T. Tateno, Characterization of stochastic bifurcations in a simple biological oscillator, J. Stat. Phys. 92 (3–4) (1998) 675–705.
[20] T. Tateno, Noise-induced effects on period-doubling bifurcation for integrate-and-fire oscillators, Phys. Rev. E (3) 65 (2) (2002) 021901,10.
[21] S. Doi, J. Inoue, S. Kumagai, Spectral analysis of stochastic phase lockings and stochastic bifurcations in the sinusoidally forced van der Pol oscillator with additive noise, J. Stat. Phys. 90 (5–6) (1998) 1107–1127.
[22] H. Poincaré, Mémoire sur les courbes définies par une équation différentielle, J. Math. Pures Appl. 1 (4) (1885) 167–244.
[23] F. Rhodes, C.L. Thompson, Rotation numbers for monotone functions on the circle, J. Lond. Math. Soc. (2) 34 (2) (1986) 360–368.
[24] J.P. Keener, Chaotic behavior in piecewise continuous difference equations, Trans. Amer. Math. Soc. 261 (2) (1980) 589–604.
[25] S. Newhouse, J. Palis, F. Takens, Bifurcations and stability of families of diffeomorphisms, Publ. Math. Inst. Hautes Études Sci. 57 (1983) 5–71.
[26] W.H. Nesse, A. Borisyuk, P.C. Bressloff, Fluctuation-driven rhythmogenesis in an excitatory neuronal network with slow adaptation, J. Comput. Neurosci. 25 (2) (2008) 317–333.
[27] F. Sagués, J.M. Sancho, J. García-Ojalvo, Spatiotemporal order out of noise, Rev. Modern Phys. 79 (2007) 829–882.
[28] A.A. Faisal, L.P.J. Selen, D.M. Wolpert, Noise in the nervous system, Nat. Rev. Neurosci. 9 (4) (2008) 292–303.
[29] B. Lindner, J. García-Ojalvo, A. Neiman, L. Schimansky-Geier, Effects of noise in excitable systems, Phys. Rep. 392 (6) (2004) 321–424.
[30] A. Destexhe, M. Rudolph, J.-M. Fellous, T. Sejnowski, Fluctuating synaptic conductances recreate in vivo-like activity in neocortical neurons, Neuroscience 107 (1) (2001) 13–24.
[31] K.K. Lin, E. Shea-Brown, L.-S. Young, Reliability of coupled oscillators, J. Nonlinear Sci. 19 (5) (2009) 497–545.
[32] A. Buonocore, A.G. Nobile, L.M. Ricciardi, A new integral equation for the evaluation of first-passage-time probability densities, Adv. Appl. Probab. 19 (4) (1987) 784–800.
[33] S. Meyn, R.L. Tweedie, Markov Chains and Stochastic Stability, second ed., Cambridge University Press, Cambridge, 2009, with a prologue by Peter W. Glynn.

[34] L. Arnold, Random Dynamical Systems, in: Springer Monographs in Mathematics, Springer-Verlag, Berlin, 1998.
[35] P. Ashwin, Minimal attractors and bifurcations of random dynamical systems, Proc. R. Soc. Lond. Ser. A Math. Phys. Eng. Sci. 455 (1987) (1999) 2615–2634.
[36] T. Kato, Perturbation Theory for Linear Operators, in: Classics in Mathematics, Springer-Verlag, Berlin, 1995, reprint of the 1980 edition.
[37] J. Glazier, A. Libchaber, Quasi-periodicity and dynamical systems: an experimentalist's view, IEEE Trans. Circuits Syst. 35 (7) (1988) 790–809.
[38] P.H. Baxendale, Statistical equilibrium and two-point motion for a stochastic flow of diffeomorphisms, in: Spatial Stochastic Processes, in: Progr. Probab., vol. 19, Birkhäuser, Boston, MA, 1991, pp. 189–218.
[39] T. Broicher, P. Malerba, A.D. Dorval, A. Borisyuk, F.R. Fernandez, J.A. White, Spike phase locking in CA1 pyramidal neurons depends on background conductance and firing rate, J. Neurosci. 32 (41) (2012) 14374–14388.
[40] T.I. Netoff, M.I. Banks, A.D. Dorval, C.D. Acker, J.S. Haas, N. Kopell, J.A. White, Synchronization in hybrid neuronal networks of the hippocampal formation, J. Neurophysiol. 93 (3) (2005) 1197–1208.
[41] G. Ermentrout, B. Beverlin II, T. Troyer, T. Netoff, The variance of phase-resetting curves, J. Comput. Neurosci. 31 (2011) 185–197.
[42] C.J. Wilson, B. Beverlin II, T.I. Netoff, Chaotic desynchronization as the therapeutic mechanism of deep brain stimulation, Front. Syst. Neurosci. 5 (50) (2011).
[43] D. Nualart, The Malliavin Calculus and Related Topics, second ed., in: Probability and its Applications (New York), Springer-Verlag, Berlin, 2006.
[44] W. Hotzel, N. Lehmkuhl, B. Werner, The spectrum of the Frobenius–Perron operator and its discretization for circle diffeomorphisms, J. Dynam. Differential Equations 14 (2) (2002) 443–461.
[45] M. Blank, G. Keller, Random perturbations of chaotic dynamical systems: stability of the spectrum, Nonlinearity 11 (5) (1998) 1351–1364.